Notes

Synthesis and Characterization of $[Ru(dpop')_2](PF_6)_2$. A Ruthenium(II) Complex with the Novel Mixed-Denticity Bridging Ligand Dipyrido-(2,3-*a*:3′,2′-*j*)phenazine (dpop′)

Ronald R. Ruminski,* Sina Underwood, Kristen Vallely, and Sandra J. Smith

Department of Chemistry, University of Colorado at Colorado Springs, Colorado Springs, Colorado 80933-7150

Received May 11, 1998

Introduction

The design and preparation of ruthenium complexes with new ligands are of great interest in light harvesting molecules.[1−5] Photophysical properties including the absorption and emission spectra, lifetimes, and electrochemical potentials of polymetallic or supramolecular ruthenium complexes are related to the structure of the bridging ligand.[1−13] Our recent research interest has been to prepare ruthenium complexes with other highly conjugated nitrogen heterocyclic ligands that can serve as stable building blocks for assembly of polymetallic light and energy storage collecting systems.[14] The dpop′ ligand(Figure 1) is of interest since it undergoes stable tridentate coordination to a central ruthenium hub in the $[Ru(dpop')_2]^{2+}$ ion, and the remote nitrogen should allow monodentate coordination to remote metal fragments in linear systems without formation of multiple structural isomers. The extended aromatic structure containing four nitrogen atoms in dpop′ should also allow for comparative red-shifted MLCT transitions and favorable electrochemical potentials for energy storage in ruthenium complexes.

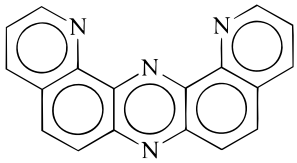

dpop'

Figure 1.

We report herein the synthesis and physical characterization of the $[Ru(dpop')_2](PF_6)_2$ complex with the bridging ligand dpop′.

Experimental Section

Reagents. All chemicals and solvents used in the synthesis were of reagent grade. Electrochemical grade tetrabutylammonium tetrafluoroborate (TBATFB) was obtained from Fluka, and tetrabutylammonium hexafluorophosphate (TBAH) was obtained from Aldrich. Argon used for deoxygenation of solutions was greater than 99.99% pure. The CD_3CN (99.95%D) and $CDCl_3$, (99.9%D) were obtained from Aldrich. Elemental analyses were performed by Atlantic Microlab, Inc. (Norcross, GA).

Physical Measurements. Ultraviolet−visible electronic absorption spectra were recorded on a Varian DMS 300 spectrophotometer. Cyclic voltammograms were recorded using a Bio Analytical Systems CV-1B cyclic voltammograph. The solvent was analytical grade CH_3CN (0.0100 M TBATFB), and potentials were recorded at a Pt electrode and are reported vs Ag/AgCl (−0.045 V vs SCE). A BAS PRW-3 electrolysis instrument and cell with a Pt gauze (Alfa Aesar) working electrode was used to generate oxidized and reduced complex metal ions. The oxidized and reduced species for UV−vis spectroelectrochemical studies were generated by bulk electrolysis of *approximately* 10^{-5} M metal complex solutions in CH_3CN/0.0100 M TBATFB and rechecked in CH_3CN/0.100 M TBAH under constant bubbling with Ar. The bulk electrolysis cell was fused on a quartz spectrophotometer cell, and absorption spectra were recorded in situ, following generation of the oxidized/reduced species. Emission spectra were recorded on a Hitachi model F-3210 fluorescence spectrophotometer with an R928 Hammamatsu detector. The instrument was fitted with a Hitachi low-temperature cell for emission at 77 K. Emission maxima are uncorrected for detector response. ^1H and ^{13}C NMR spectra of the $[Ru(dpop')_2]^{2+}$ ion were recorded in CD_3CN on a Varian Inova 500 MHz spectrometer at CU—Boulder, and spectra of dpop′ were recorded on a Varian Mercury 200 MHz spectrometer at CU—Colorado Springs.

Synthesis. The mixed denticity ligand dpop′ was prepared according to the literature[15] with minor modifications.[16] The nitration of phenazine was carried out at 80 °C rather than 100 °C to avoid excessive oxidation of phenazine, and cyclization of the 1,9-dihydrophenazine was achieved at 120 °C rather than 145 °C. Anal. Calcd for $C_{18}H_{10}N_4 \cdot 2H_2O$ (318.32 g/mol): C, 67.91; H, 4.44; N, 17.59. Found: C, 68.02; H, 4.46; N, 17.55. Average yield 14% [lit. 6% $C_{18}H_{10}N_4 \cdot 1.5H_2O$].

$[Ru(dpop')_2](PF_6)_2 \cdot 2H_2O$. A sample of 0.0951 g ($2.99 \times 10^{-4}$ mol) of dpop′ and 0.0247 g (1.19×10^{-4} mol) of $RuCl_3$ was mixed in 20 mL of ethylene glycol and heated at reflux for 30 min. The crude red product was precipitated by addition of an equal volume of aqueous NH_4PF_6 to the cooled solution and collected by vacuum filtration. After

(1) Roundhill, D. M. *Photochemistry and Photophysics of Metal Complexes*; Plenum Press: New York, 1994.
(2) Scandola, F.; Bignozzi, C. A. *Photosensitization and Photocatalysis Using Inorganic and Organometallic Compounds*; Kluwer Academic Publishers: Dordrecht, The Netherlands, 1993; pp 161−216.
(3) Balzani, V., Ed. *Supramolecular Photochemistry*; NATO ASI Series C214; Reidel: Dordrecht, The Netherlands, 1987.
(4) Fox, M. A., Chanon, M., Eds. *Photoinduced Electron Transfer*; Elsevier: New York**,** 1988.
(5) Juris, A.; Barigelletti, S.; Campagna, S.; Balzani, V.; Belser, P.; von Zelewski, A. *Coord. Chem. Rev.* **1988**, *84*, 85.
(6) Anderson, P. A.; Strouse, G, F.; Treadway, J. A.; Keene, F. R.; Meyer, T. J. *Inorg. Chem.* **1994**, *33*, 3863.
(7) Murphy, W. R., Jr.; Brewer, K. J.; Gettliffe, G.; Petersen, J. D. *Inorg. Chem.* **1989**, *28*, 81.
(8) Denti, G.; Campagna, S.; Sabatino, L.; Serroni, S.; Ciano, M.; Balzani, V. *Inorg. Chem.* **1990**, *29*, 4750.
(9) Strouse, G. F.; Schoonover, J. R.; Duesing, R.; Boyde, S.; Jones, J. E., Jr.; Meyer, T. J. *Inorg. Chem.* **1995**, *34*, 473.
(10) Treadway, J. A.; Loeb, B.; Lopez, R.; Anderson, P. A.; Keene, F. R.; Meyer, T. J. *Inorg. Chem.* **1996**, *35*, 2242.
(11) Denti, G.; Campagna, S.; Serroni, S.; Ciano, M.; Balzani, V. *J. Am. Chem. Soc.* **1992**, *114*, 2944.
(12) Masschelein, A.; Kirsch-De Mesmaker, A.; Verhoeven, C., Nasielski-Hinkens, R. *Inorg. Chim. Acta* **1987**, *129*, L13.
(13) Bolger, J.; Gourdon, A.; Ishow, E.; Launay, J.-P. *Inorg. Chem.* **1996**, *35*, 2937.
(14) Ruminski, R. R.; Deere, T. P.; Olive, M.; Serveiss, D. *Inorg. Chim. Acta* **1998** *281*, 1.
(15) Pfeiffer, F. R.; Case, F. H. *J. Org. Chem.* **1966**, *31*, 3384.
(16) Ruminski, R. R.; DeGroff, C.; Smith, S. J. *Inorg. Chem.* **1992**, *31*, 3325.

10.1021/ic980530k CCC: $15.00
Published on Web 11/12/1998

Table 1. Electrochemical and Electronic Absorption Data for $[Ru(dpop')_2]^{2+}$ and Similar Ru^{2+} Complexes

species	λ nm (ϵ M^{-1} cm^{-1})	assignment	$E_{1/2}$ $Ru^{2+/3+}$	$E_{1/2}$ $L^{0/-}$	$E_{1/2}$ $L^{-/-2}$	reference
$[Ru(dpop')_2]^{2+}$	517 (25.0)	MLCT	1.74[a]	−0.51; −0.79	−1.39; −1.65	this work
	422 (5.0)					
	356 (44.0)	MLCT				
	340 (sh)	IL				
	306 (110)	IL				
	271 (41)	IL				
$[Ru(terp)_2]^{2+}$	478 (14.3)	MLCT	1.27[b]	−1.27; −1.51		18, 17
$[Ru(tpp)_2]^{2+}$	475 (∼23)	MLCT	1.54[b]	−0.83; −1.07		18
$[Ru(bpm)_3]^{2+}$	454 (8.6)	MLCT	1.69[c]	−0.91; −1.08; −1.28		19, 20
	418 (8.2)	MLCT				
	332	MLCT				
$[Ru(bpy)_3]^{2+}$	452 (14.5)	MLCT	1.27[c]	−1.31; −1.50; −1.77		13, 19
	345 (6.5)	MLCT				
	285 (87)	IL				
$[Ru(bpy)_2(tpphz)]^{2+}$	450 (19.7)	MLCT	1.33[b]	−0.88; −1.33; −1.51		18
	380 (33.9)					
	361 (24.1)					
	284 (133)					
$[Ru(bpy)_2(hat)]^{2+}$	484 (sh), 432 (10)	MLCT	1.56[b]	−0.84		12

[a] In CH_3CN vs Ag/AgCl. [b] In CH_3CN vs SCE. [c] In CH_3CN vs SSCE.

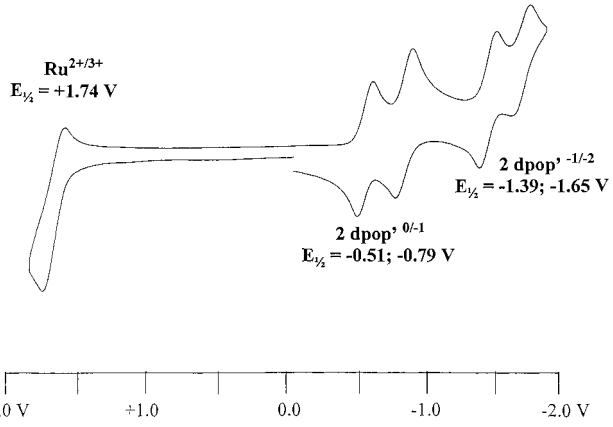

Figure 2. Cyclic voltammogram and electrochemical potentials vs Ag/AgCl for $[Ru(dpop')_2]^{2+}$ in acetonitrile/0.0100 M TBATFB.

air-drying, the product was washed with $CHCl_3$ to remove excess dpop′. The $[Ru(dpop')_2](PF_6)_2 \cdot 2H_2O$ product was purified by elution from an Al_2O_3 column with a 1.0 g of NH_4PF_6/1 L of acetone mixture, followed by rotary evaporation to a minimum volume and precipitation with ether. After it was washed with a minimum volume of water to remove any excess NH_4PF_6, the product was vacuum-dried at 60 °C overnight. Anal. Calcd for $[Ru(dpop')_2](PF_6)_2 \cdot 2H_2O$ (991.61 g/mol): C, 43.60; H, 2.44; N, 11.29. Found: C, 43.61; H, 2.42; N, 11.36. Weight product: 0.0921 g (9.29×10^{-5} mol), 78% yield.

Results and Discussion

The $[Ru(dpop')_2](PF_6)_2 \cdot 2H_2O$ compound is air stable and soluble in a variety of solvents including acetonitrile, acetone, and water (slightly).

The cyclic voltammogram of $[Ru(dpop')_2]^{2+}$ ion is recorded in CH_3CN (Figure 2) and displays a reversible $Ru^{2+/3+}$ redox couple at +1.74 V vs Ag/AgCl. The potential is more positive than for homoleptic monometallic Ru^{2+} complexes with similar polypyridyl ligands such as 2,2′:6′,2″-terpyridine (trpy),[17] 2,3,5,6-tetrakis(2-pyridyl)pyrazine (tpp),[18] 2,2′-bipyrimidine (bpm),[19,20] and 2,2′-bipyridine (bpy),[13,19,20] and this result indicates that the Ru^{2+} dπ−dpop′ pπ* back-bonding interaction is stronger than in previous complexes (Table 1). The oxidation potential is also more positive than for heteroleptic $[(bpy)_2Ru(L-L)]^{2+}$ complexes with L−L = dipyrazido[2,3-*f*:2′,3′-*h*]quinoxaline (hat)[12] and tetrapyrido[3,2-*a*:2′,3′-*c*:3″,2″-*h*:2‴,3‴-*j*]phenazine (tpphz);[13] however, a direct comparison of Ru^{2+} dπ−L−L pπ* back-bonding interaction cannot be made since the HOMO contains large contributions from the bpy pπ* as well as L−L pπ* orbital. The cyclic voltammogram of $[Ru(dpop')_2]^{2+}$ also shows a pair of reversible reductions at −0.51 and −0.79 V, and another pair of reductions at −1.39 and −1.65 V. Based on the comparative peak currents with the $Ru^{2+/3+}$ process, these are attributed to four individual one-electron processes. The reductions at −0.51 and −0.79 V are attributed to two dpop′$^{0/-}$ processes, and the reductions at −1.39 and −1.65 V are attributed to two dpop′$^{-/-2}$ processes.

The absorption spectrum of $[Ru(dpop')_2]^{2+}$ in CH_3CN displays several intense absorptions throughout the visible−UV spectrum (Figure 3, Table 1). Assignment of transitions is aided by examination of spectral changes that occur upon oxidation and reduction of $[Ru(dpop')_2]^{2+}$ and dpop′ (Figures 3−5). (A table of absorption data for $[Ru(dpop')_2]^{3+,2+,+,0}$ and dpop′ $^{0,-,-2}$ is deposited as Supporting Information.)

The absorption spectra of $[Ru^{3+}(dpop')_2]^{3+}$; $[Ru(dpop')(dpop'^{-})]^{+}$ and $[Ru(dpop'^{-})_2]$ (Figures 3,4) were recorded following oxidation or reduction of a sample of $[Ru(dpop')_2]^{2+}$, in situ, at the appropriate potentials in the sequence shown below.

$$[Ru^{3+}(dpop')_2]^{3+} \underset{e^-}{\overset{+1.85\ V}{\rightleftharpoons}} \underset{\textit{initial solution}}{[Ru(dpop')_2]^{2+}} \underset{e^-}{\overset{-0.60\ V}{\rightleftharpoons}} [Ru(dpop')(dpop'^{-})]^{+} \underset{e^-}{\overset{-1.00\ V}{\rightleftharpoons}} [Ru(dpop'^{-})_2]$$

All steps were found to occur in excess of 90% reversibility when the samples were rigorously deoxygenated, as estimated from the regeneration of the initial absorption spectrum. The absorption spectra of dpop′ and dpop′$^{-}$ (Figure 5) were also recorded. The reversibility of dpop′-based reductions was extremely oxygen sensitive.

Consideration of the absorption spectrum of $[Ru(dpop')_2]^{2+}$ and dpop′, spectroelectrochemical results, and previous inter-

(17) Berger, R.; McMillin, D. R. *Inorg. Chem.* **1988**, *27*, 4245.
(18) Thummel, P. R.; Chirayil, S. *Inorg. Chim. Acta* **1988** *154*, 77.
(19) Rillema, D. P.; Allen, G.; Meyer, T. J. Conrad, D. *Inorg. Chem.* **1983**, *22*, 1617.
(20) Sahai, R.; Morgan, L.; Rillema, D. P. *Inorg. Chem.* **1988**, *27*, 3495 (Table 2).

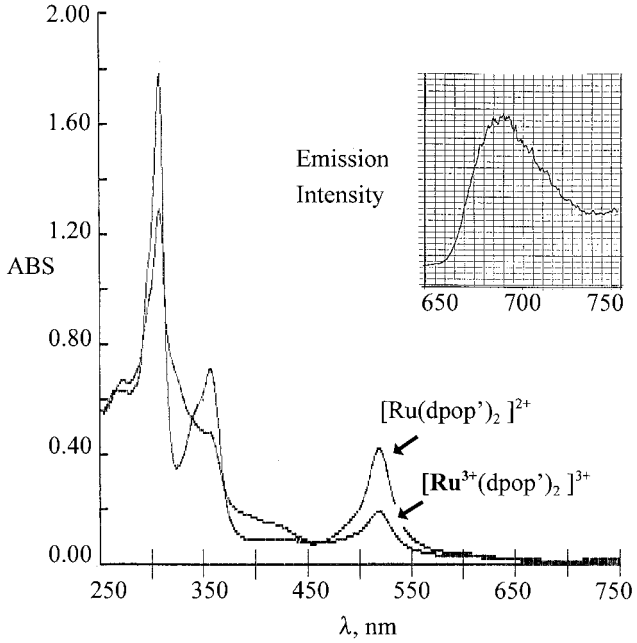

Figure 3. Electronic absorption spectra of 1.65×10^{-5} M [Ru(dpop′)$_2$]$^{2+}$ and oxidized [Ru(dpop′)$_2$]$^{3+}$ ions in CH_3CN (0.0100 M TBATFB) at 24 °C in 1 cm path length quartz cell. Inset is the emission spectrum of [Ru(dpop′)$_2$]$^{2+}$ at 77 K in 4:1 EtOH/MeOH glass.

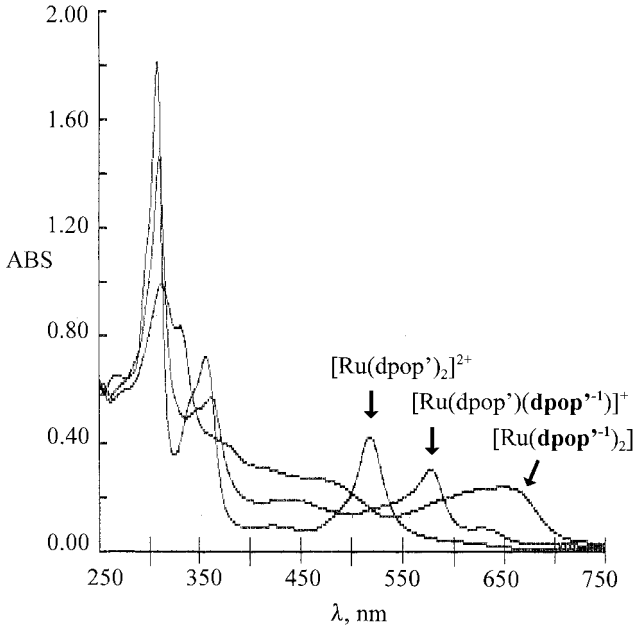

Figure 4. Electronic absorption spectra of 1.65×10^{-5} M [Ru(dpop′)$_2$]$^{2+}$ and reduced [Ru(dpop′)$_2$]$^{+,0}$ species in CH_3CN (0.0100 M TBATFB) at 24 °C in 1 cm path length quartz cell.

pretations of spectra of similar complexes leads us to the following assignments for [Ru(dpop′)$_2$]$^{2+}$ and the oxidized and reduced species.

The lowest-energy absorption of [Ru(dpop′)$_2$]$^{2+}$ at 517 nm and the low-energy tail near 600 nm are attributed to Ru^{2+} dπ → dpop′π* MLCT transitions due to the low energy of the transition, the loss of intensity after $Ru^{2+/3+}$ oxidation, and by analogy to numerous Ru(II) complexes including [Ru(trpy)$_2$]$^{2+}$ and [Ru(tpp)$_2$]$^{+2}$.[13,18] It is surprising that the absorption spectrum of the oxidized [Ru(dpop′)$_2$]$^{3+}$ complex displays a peak at 516 nm (a spectroelectrochemical time-based plot is deposited as Supporting Information). Oxidation at +1.85 V was continued until the absorption spectrum remained constant, and the

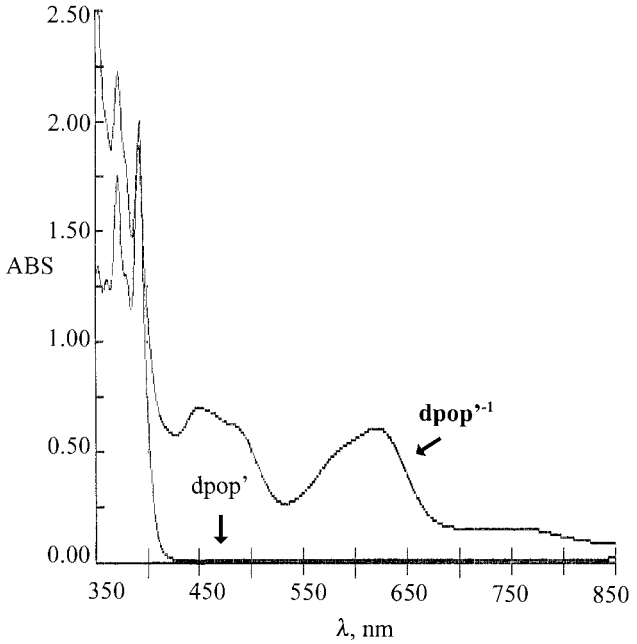

Figure 5. Electronic absorption spectra of dpop′ and dpop′$^-$ species in CH_3CN (0.0100 M TBATFB) at 24 °C in 1 cm path length quartz cell.

spectrum consistently displays a peak at 516 nm. An exhaustive (12 h) oxidation of [Ru(dpop′)$_2$]$^{2+}$ at +2.00 V does produce almost complete loss of the 516 nm absorption; however, the subsequent re-reduction is completely irreversible and is most likely the result of a secondary reaction. The absorption at 516 nm after [Ru(dpop′)$_2$]$^{2+/3+}$ oxidation could be the result of a new dpop′π → Ru^{3+} dπ transition, as has previously been suggested following $Ru^{2+/3+}$ oxidation of polymetallic complexes.[21] The weak absorption maximum at 422 nm lies outside the energy generally observed for Ru^{2+} d−d ligand field transitions in [Ru(bpy)$_3$]$^{2+}$ and [Ru(NH$_3$)$_6$]$^{2+}$ ions,[1] and at this time the results do not allow a definitive assignment to this weak transition. The 356 nm absorption peak of [Ru(dpop′)$_2$]$^{2+}$ is attributed primarily to a higher energy Ru^{2+}dπ → dpop′ π* CT transition also due to it's loss upon $Ru^{2+/3+}$ oxidation. The $Ru^{2+/3+}$ oxidation also decreases absorption intensity at 306 nm; however, the peak remains unchanged in energy and shape near the wavelength maximum. The shoulder near 350 nm and peak at 306 nm remaining after $Ru^{2+/3+}$ oxidation (Figure 3) indicate that dpop′ intraligand (IL) transitions underlie this region of the spectrum of [Ru(dpop′)$_2$]$^{2+}$. This is supported by inspection of the absorption spectrum (Figure 5) of uncomplexed dpop′ [15] which displays several dpop′ IL transitions between 400 and 350 nm and an intense dpop′π → π* IL transition at 300 nm. On this basis, the absorption peak at 306 nm for [Ru(dpop′)$_2$]$^{2+}$ is assigned to a dpop′ π → π* IL transition while the shoulder near 340 nm to other dpop′ IL transitions that overlap with the high energy Ru^{2+} dπ → dpop′ π* CT transition at 356 nm.

Reduction of [Ru(dpop′)$_2$]$^{2+}$ (Figure 4) produces absorptions near 625, 575, and 440 nm for the [Ru(dpop′)(dpop′$^-$)]$^+$ ion and at 650 and 460 nm for the [Ru(dpop′$^-$)$_2$] complex. By comparison with the absorption spectrum of the dpop′$^-$ ion (Figure 5), the peaks near 650 and 450 nm are assigned to new dpop′$^-$ π* → dpop′$^-$$\pi$* IL transitions in the reduced complexes. The absorption spectrum of [Ru(dpop′)(dpop′$^-$)]$^+$ also displays an absorption at 575 nm which is assigned to the

(21) Bridgewater, J. S.; Vogler, L. M.; Molnar, S. M.; Brewer, K. J. *Inorg. Chem. Acta* **1993**, *208*, 179.

Table 2. NMR Data for $[Ru(dpop')_2]^{2+}$ and dpop′

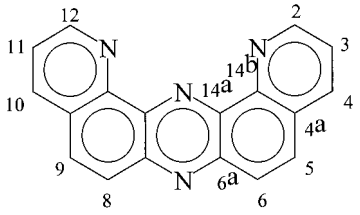

species	H_2	H_3	H_4	H_5	H_6	$J_{2,3}$	$J_{2,4}$	$J_{3,4}$	$J_{5,6}$
dpop′	9.48	7.92	8.51	8.28	8.38	4.6	1.6	8.0	9.0
$[Ru(dpop')_2]^{2+}$	7.60	7.34	8.53	8.59	8.75	8.0	1.0	5.4	9.5
	C_2	C_3	C_4	C_{4a}	C_5	C_6	C_{6a}	C_{14a}	C_{14b}
$[Ru(dpop')_2]^{2+}$	158.28	127.68	138.56	131.89	134.46	130.08	142.17	151.33	147.54

remaining Ru^{2+} $d\pi \rightarrow$ dpop′ π^* CT transition. The comparatively lower Ru^{2+} $d\pi \rightarrow$ dpop′ π^* CT energy of the reduced complex can be explained by a destabilized set of $Ru^{2+}d\pi$ orbitals when simultaneously coordinated to the dpop′ $^-$ ligand. The spectrum of the doubly reduced $[Ru(dpop'^{-})_2]$ complex shows no absorptions associated with a low-lying Ru^{2+} $d\pi \rightarrow$ dpop′ π^* CT transition. The changes in the absorption spectra of the $[Ru(dpop')_2]^{2+,+,0}$ species follows a similar pattern previously established for the reduced $[Ru(trpy)_2]^{2+,+,0}$ series.[17]

Samples of $[Ru(dpop')_2]^{*2+}$ in 4EtOH/MeOH glass at 77 K were found to emit at 690 nm following excitation into the lowest-energy MLCT absorption at 517 nm (Figure 3 (inset)). No emission was detectable from room-temperature deoxygenated samples of $[Ru(dpop')_2]^{*2+}$ in CH_3CN, 4EtOH/MeOH, CH_2Cl_2, THF, or acetone. The absence of room-temperature emission from $[Ru(dpop')_2]^{*2+}$ in solvents of low Guttman AN and dielectric constants suggests that solvent interaction with the noncoordinated N on the central pyrazine ring is not a primary deactivation pathway. The emission behavior of $[Ru(dpop')_2]^{*2+}$ is similar to that of $[Ru(trpy)_2]^{*2+}$, which also emits in 4EtOH/MeOH glass at 77 K[22] but is nonemissive in room-temperature solution.[17,23−25] The lack of room-temperature emission from $[Ru(trpy)_2]^{*2+}$ has been attributed to an effective nonradiative decay path due to an open structure of the excited state which permits excited state−solvent interaction,[23] and a wide bite angle of the three pyridine rings producing a relatively weak ligand field and allowing for rapid d−d quenching of the MLCT excited state.[24,25] The lower-energy MLCT state of $[Ru(dpop')_2]^{2+}$, and the rigid structure of dpop′ prohibiting large molecular distortions associated with the d−d state would be expected to reduce MLCT−dd interactions compared with $[Ru(trpy)_2]^{2+}$.

The ^1H, ^{13}C, and $^1H-^{13}C$ correlation NMR spectra of $[Ru(dpop')_2]^{2+}$ were recorded, and the ^1H and ^{13}C results are summarized in Table 2 (spectra are deposited as Supporting Information). The clear pattern of five sets of proton and nine carbon resonances is consistent with equivalent coordination of the dpop′ ligands in octahedral geometry. The ^{13}C NMR spectrum displays five intense signals from the protonated carbons and four less intense signals from the deprotonated carbons, as confirmed by the $^{13}C-^1H$ correlation spectrum. Of interest is the large upfield shift of 1.88 ppm δ that is observed for H_2 upon complexation. Previous assignments[26] in the downfield position of the carbon adjacent to the nitrogen, in conjunction with the $^{13}C-^1H$ correlation spectrum, confirms the doublet resonance at 7.60 ppm with H_2, and the doublet resonance at 8.53 ppm with H_4 on the $[Ru(dpop')_2]^{2+}$ ion. The upfield shift is the result of H_2 being directed in the shielding region of the orthogonal dpop′ in $[Ru(dpop')_2]^{2+}$. This effect has previously been studied for a series of annelated terpyridine ruthenium complexes.[27]

We are currently involved with the preparation of polymetallic complexes centered around the $[Ru(dpop')_2]^{2+}$ unit.

Acknowledgment. We acknowledge a Gates Foundation Grant administered by the Research Corporation for partial funding of this work.

Supporting Information Available: A table of absorption wavelength data for $[Ru(dpop')_2]^{+3,+2,+,0}$ and dpop′ $^{0,-,-2}$ shown in Figures 3−5 is deposited as Supporting Information. A figure of the changing absorption spectrum of $[Ru(dpop')_2]^{+2/+3}$, as a function of electrolysis time at +1.85 V until no further absorption change is observed, is also presented. Figures of the ^1H, ^{13}C, and $^1H-^{13}C$ correlation NMR spectra of $[Ru(dpop')_2]^{2+}$ are also deposited. Ordering information is given on any current masthead page.

IC980530K

(22) Demas, J. N.; Crosby, G. A. *J. Mol. Spectrosc.* **1968**, *26*, 72.
(23) Young, R. C.; Nagle, J. K., Meyer, T. J.; Whitten, D. G. *J. Am. Chem. Soc.* **1978**, *100*, 4773.
(24) Kirchoff, J. R.; McMillin, D. R.; Marnot, P. A.; Sauvage, J.-P. *J. Am. Chem. Soc.* **1985**, *107*, 1138.
(25) Calvert, J. M.; Casper, J. V.; Binstead, R. A.; Westmoreland, T. D.; Meyer, T. J. *J. Am. Chem. Soc.* **1982**, *104*, 6620.
(26) Memory, J. A.; Wilson, N. K. *NMR of Aromatic Compounds*; Wiley: New York, 1982.
(27) Thummel, R. A.; Jahng, Y. *Inorg. Chem.* **1986**, *25*, 2527.